RESEARCH ARTICLE SUMMARY

PLANT SCIENCE

A conserved superlocus regulates above- and belowground root initiation

Moutasem Omary†, Naama Gil-Yarom†, Chen Yahav, Evyatar Steiner, Anat Hendelman, Idan Efroni*

INTRODUCTION: Plants continuously adjust their body plans to adapt to the local environment by forming new organs in different developmental contexts. Underground, lateral roots initiate from designated cells in the pericycle of the main root. Aboveground, plants generate shoot-borne roots, bypassing the embryonic root-shoot lineage separation. Shoot-borne roots commonly form in response to stimuli such as flooding or wounding, but many plants also initiate these roots as part of their normal development. Indeed, fossil record evidence suggests that growth by shoot-bearing roots is an ancestral trait of flowering plants (angiosperms). However, the ontogeny of shoot-borne roots and its relationship to the initiation of lateral and wound-induced roots are unclear.

RATIONALE: Tomato (*Solanum lycopersicum*) is a vine that readily generates many roots from its stem as part of its normal development, making it an attractive model system with which to study shoot-borne root initiation. Here, we characterized the ontogeny of tomato shoot-borne roots at single-cell resolution. We used these data to identify a key regulator of shoot-borne root initiation and applied genetic and molecular characterization to multiple angiosperm species to test the functional and regulatory conservation of shoot-borne and lateral root initiation programs.

RESULTS: To identify the origin of shoot-borne roots, we generated tomatoes carrying fluorescent reporters for early root initiation transcriptional responses. Using these, we show that tomato shoot-borne roots initiate from a small population of primary phloem–associated cells. We isolated these rare cells for single-cell mRNA-sequencing profiling, along with three other time points of shoot-borne root development. This analysis uncovered the existence of a transition state unique to the earliest stage of root meristem initiation. Trajectory reconstruction indicated that cells in this state were the progenitors of the new root stem cells and cap tissues.

The transition state was characterized by the expression of a *LATERAL ORGAN BOUNDARIES DOMAIN* (*LBD*) transcription factor that we named *SHOOT BORNE ROOTLESS* (*SBRL*) because loss of function of this gene resulted in plants lacking shoot-borne roots. High-resolution phylogenetic analysis of the *SBRL* family revealed that it belongs to an angiosperm-specific gene clade (subclass IIIB). We show that members of this clade had shoot-borne root–specific expression or function in multiple species (potato, *Arabidopsis*, sweet potato, white beans, and sorghum). Further, previously identified regulators of shoot-borne root initiation in maize and rice were also classified as subclass IIIB genes, indicating that the shoot-borne root–specific function of this gene is deeply conserved.

Comparative genomics identified that subclass IIIB genes are part of a conserved superlocus containing genes of the sister clade, subclass IIIA. Although subclass IIIA genes did not play a role in shoot-borne root initiation, we show that they control the initiation of underground lateral roots in multiple plant species. Similar to the function of subclass IIIB in shoot-borne roots, the expression of subclass IIIA genes was transient and correlated with the expression of transition state markers, suggesting a common mechanism for root meristem initiation.

Apart from naturally occurring shoot-borne roots, plants also form wound-induced roots. Genetic analysis identified at least two classes of these roots: The first is derived from stems and regulated by the subclass IIIB gene *SBRL*, and the second is derived from hypocotyl wound tissue and regulated by a subclass IIIA gene.

The conserved root-type-specific function of subclass IIIA and IIIB genes suggested that their regulatory program may be ancient. Indeed, the superlocus had a high level of noncoding sequence conservation, and tomato regulatory sequences were sufficient to drive transient shoot-borne- and lateral-root-specific expression even when used in the distant *Arabidopsis*.

Finally, to test whether this family regulates the initiation of all root types, we generated a tomato loss-of-function mutant for all three subclass IIIA/IIIB genes found in this species. These triple mutants lacked shoot-borne, lateral, and wound-induced roots, producing only a single barren embryonic root.

CONCLUSION: We conclude that root meristem formation initiates through a common transition state associated with deeply conserved subclass IIIA and IIIB genes. These genes control the initiation of different root types, with subclass IIIB playing a nonredundant role in shoot-borne root initiation and subclass IIIA acting in the initiation of lateral and some wound-induced roots. The appearance of a superlocus of subclass IIIA and IIIB genes in early angiosperm allowed specialization in the genetic regulation of different root types, enabling the plant's complex developmental response to varied environments. ■

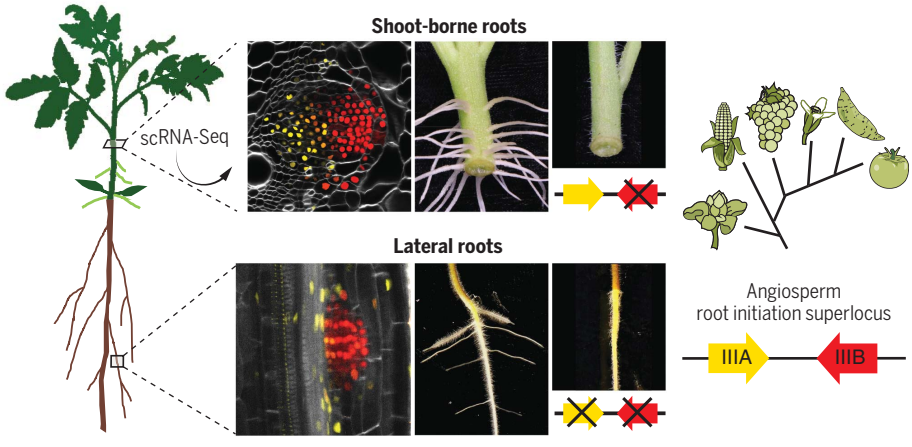

Conserved regulation of root initiation. The initiation of tomato shoot-borne and lateral roots varies in developmental and hormonal dynamics. However, single-cell RNA-sequencing (scRNA-Seq) of shoot-borne roots revealed that they share a common transition state. An angiosperm-specific superlocus of transition-state-expressed genes governs root initiation, with the two superlocus members (subclass IIIA and IIIB genes) having conserved root-type-specific activity.

ART CREDIT: MOUTASEM OMARY

The list of author affiliations is available in the full article online.
*Corresponding author. Email: idan.efroni@mail.huji.ac.il
†These authors contributed equally to this work.
Cite this article as M. Omary *et al.*, *Science* **375**, eabf4368 (2022). DOI: 10.1126/science.abf4368

READ THE FULL ARTICLE AT
https://doi.org/10.1126/science.abf4368

RESEARCH ARTICLE

PLANT SCIENCE

A conserved superlocus regulates above- and belowground root initiation

Moutasem Omary[1]†, Naama Gil-Yarom[1]†, Chen Yahav[1], Evyatar Steiner[2], Anat Hendelman[3], Idan Efroni[1]*

Plants continuously form new organs in different developmental contexts in response to environmental cues. Underground lateral roots initiate from prepatterned cells in the main root, but cells can also bypass the root-shoot trajectory separation and generate shoot-borne roots through an unknown mechanism. We mapped tomato (*Solanum lycopersicum*) shoot-borne root development at single-cell resolution and showed that these roots initiate from phloem-associated cells through a unique transition state. This state requires the activity of a transcription factor that we named *SHOOTBORNE ROOTLESS* (*SBRL*). Evolutionary analysis reveals that *SBRL*'s function and cis regulation are conserved in angiosperms and that it arose as an ancient duplication, with paralogs controlling wound-induced and lateral root initiation. We propose that the activation of a common transition state by context-specific regulators underlies the plasticity of plant root systems.

The body of vascular plants is divided into the root and shoot. Roots are formed through the activity of root meristems, which contain tissue-specific stem cells, or initials, arranged around slowly dividing quiescent cells and protected by the root cap (*1*). The primary root meristem is formed from the basal part of the embryo (*2*). After embryogenesis, lateral root meristems initiate from the pluripotent pericycle tissue of the primary root (*3*). Lateral root initiation is patterned by a periodic oscillatory mechanism that integrates auxin responses, root growth rates, localized cell wall modifications, and chemical signals to prime specific pericycle cells (*4*–*9*). Although the root-shoot lineages separate early during embryogenesis, most plants can also initiate shoot-borne roots to form multiple independent root systems. Reflecting the conceptual separation between the lineages, these roots are commonly referred to as "adventitious," meaning "in the wrong place" (*10*). However, shoot-borne roots arise as part of the normal development of many plants, and according to the fossil record, root-bearing shoots were the dominant body plan of early angiosperms (*11*). Botanists distinguish between adventitious roots such as those induced by wounds and naturally occurring shoot-borne roots (*12*); however, little is known about the initiation of these roots, their tissue of origin is disputed, and the ontogenetic relationships among shoot-borne, lateral, and wound-induced roots are unclear (*13*, *14*).

Two plant hormones, auxin and cytokinin, play a key role in root initiation. Auxin response is activated in lateral root meristem progenitors, whereas response to cytokinin marks their flanking cells (*15*, *16*). Auxin triggers multiple downstream processes, including promotion of cell growth and mitotic cell division, through the activation of *LATERAL ORGAN BOUNDARIES DOMAIN* (*LBD*) transcription factors (*17*). Other auxin-induced transcription factors, such as members of the *PLETHORA/AINTEGUMENTA* family (*18*), are required for the establishment of proper cell division patterns and, at later stages, for the acquisition of specific cell fates (*19*, *20*).

Scarce evidence from monocots, in which shoot-borne roots form the bulk of the root system, suggests that similar genes may play a role in both shoot-borne and lateral root initiation. In maize and rice, shoot-borne root initiation requires the auxin-induced *LBD* transcription factors *ROOTLESS CONCERNING CROWN AND SEMINAL ROOT* (*RTCS*) and *CROWN ROOTLESS1* (*CRL1*), respectively (*21*–*23*), as well as the *PLETHORA/AINTEGUMENTA* (*PLT*) family protein *CRL5* (*24*). Not all gene families are shared between root types, however, because the WUSCHEL-like *WOX11* is specifically required for shoot-borne root development (*25*). The common model plant *Arabidopsis thaliana* lacks stem elongation and only rarely produces shoot-borne roots from its hypocotyl. Thus, to study dicot shoot-borne root initiation at high resolution, we turned to tomato (*Solanum lycopersicum*), a vine that naturally generates a large number of roots from easily accessible stems (Fig. 1, A to J).

Shoot-borne roots initiate from phloem-associated cells

Under our growth conditions, shoot-borne roots were observed on the first tomato internode 7 days after cessation of internode elongation (fig. S1, A and B). Roots continuously initiated from young internodes, forming a developmental gradient such that older internodes had more developed roots (Fig. 1, B to J). Anatomically, the stem is composed of an external epidermal layer, several layers of large cortex cells, and a layer of elongated starch-sheath cells containing starch granules. Internal to these is the vasculature tissue, the phloem with embedded phloem fibers (or pericyclic fibers), sieve cells, and accompanying companion cells. Further internal to the phloem are the cambium and xylem layers surrounding the stem pith (Fig. 1A and fig. S1, C to E). Shoot-borne roots formed at the vasculature tissue region and were preferentially located at the edge of vascular bundles (fig. S1, F and G). To study events before the activation of cellular proliferation, we generated a tomato carrying a dual-color transcriptional reporter for auxin (DR5) (*26*) and cytokinin (TCSn) (*27*) response (*DR5:mScarleti-NLS TCSn:mNeonGreen-NLS*). Before root meristem initiation, we observed sporadic expression of TCSn in the distal region of the phloem (Fig. 1K). In ~4-week-old plants, immediately after the cessation of internode elongation, root initiation events, which were marked by the induction of both auxin and cytokinin signaling in a group of 21 ± 4.4 cells, were observed in enlarged primary phloem parenchyma cells (Fig. 1L and fig. S1H). Subsequently, the expression of auxin and cytokinin response reporters separated into two domains, resembling a mature meristem, although regions of overlap remained (Fig. 1, M to P, and fig. S1I). We observed similar dynamics in tomatoes carrying the sensitive auxin response marker *pIAAmotif* (*28*) (fig. S1, J to N). These events were used to define five stages of shoot-borne root formation: (i) TCS induction, (ii) DR5/TCS coexpression, (iii) expression domain expansion, (iv) primordia entry into cortex, and (v) DR5/TCS domain separation and mature meristem (Fig. 1, K to P). In *Arabidopsis*, a transient overlap of the auxin-cytokinin response was reported to occur during embryonic root meristem initiation (*29*) but not during lateral root initiation (*15*, *16*). These hormonal dynamics were conserved in tomato, with initial lateral root cells marked by auxin response and flanked by cytokinin response–expressing cells (Fig. 1, Q to V), whereas in the tomato embryo, both auxin and cytokinin responses overlapped at the basal part, followed by domain separation (fig. S2, A to E). Overall, this shows that shoot-borne roots initiate from differentiated primary phloem parenchyma cells

[1]The Institute of Plant Science and Genetics in Agriculture, Faculty of Agriculture, The Hebrew University of Jerusalem, Rehovot, Israel. [2]Department of Plant Sciences, Weizmann Institute of Science, Rehovot, Israel. [3]Cold Spring Harbor Laboratory, Cold Spring Harbor, NY, USA.
*Corresponding author. Email: idan.efroni@mail.huji.ac.il
†These authors contributed equally to this work.

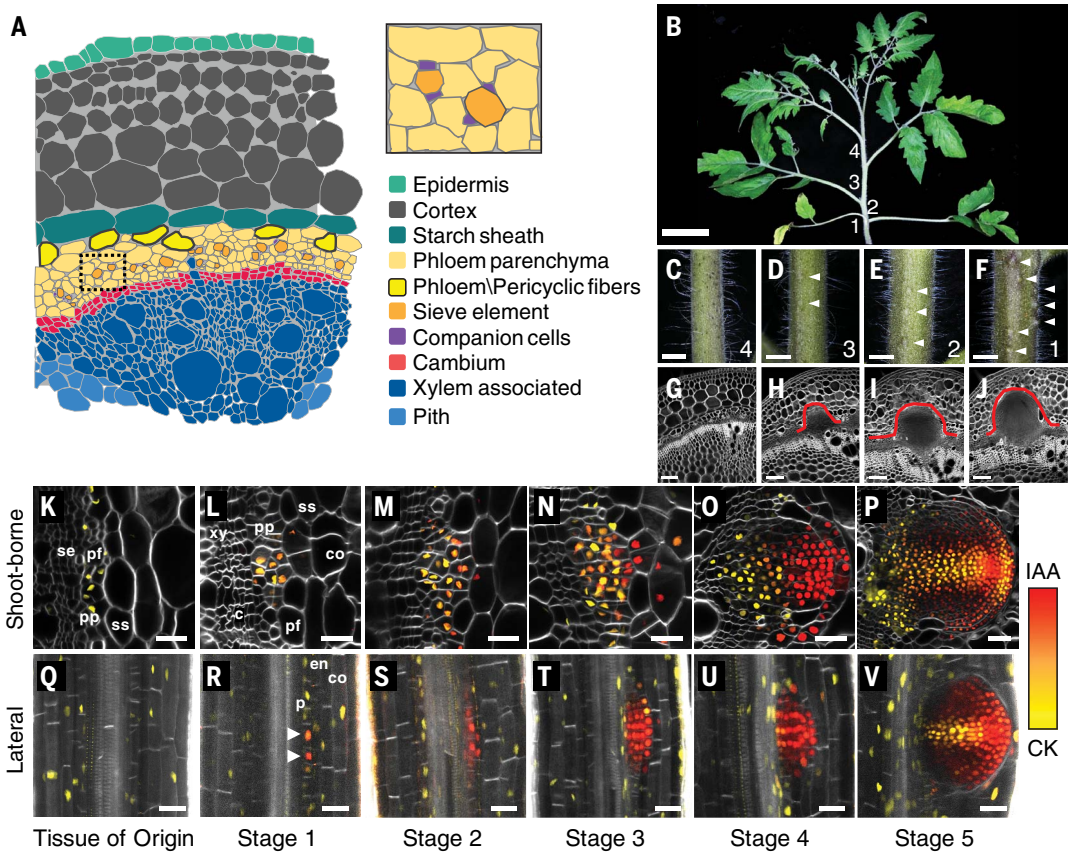

Fig. 1. Shoot-borne and lateral root formation in tomato. (**A**) Two-dimensional illustration of the different cell types in the tomato stem and their spatial organization. Inset shows a magnification of the phloem region. (**B**) Eight-week-old tomato plant. (**C** to **J**) Close-up [(C) to (F)] and confocal images of cross-sections [(G) to (J)] of numbered internodes of the plant in (B) from young [(C) and (G)] to old [(F) and (J)]. Arrowheads in (D) to (F) indicate initiating shoot-borne roots. Red lines in (H) to (J) mark the root primordia. (**K** to **V**) Confocal images of *DR5:mScarleti-NLS TCSn:mNeonGreen-NLS* plants showing auxin (red) and cytokinin (yellow) responses at the different stages of shoot-borne [(K) to (P)] or lateral [(Q) to (V)] root development at corresponding developmental stages. Scale bars: (B), 5 cm; (C) to (F), 1 cm; (G) to (J), 50 μm; and (K) to (V), 25 μm. c, cambium; xy, xylem; pp, phloem parenchyma; pf, phloem/pericyclic fibers; se, sieve element; co, cortex; ss, starch sheath; p, pericycle; en-endodermis.

with an initiation program that distinguishes it from lateral roots.

Single-cell profiling reveals transitional cell state

To follow the trajectories of phloem parenchyma cells as they form root meristems, we generated single-cell mRNA-sequencing profiles of stage 1, 3 and 5 root meristems and from phloem-associated tissue of origin before root initiation. To isolate these very rare tissues, we staged and microdissected individual initiation events under a microscope, followed by cell disassociation and sorting based on hormonal response reporters using fluorescence-activated cell sorting (FACS; TCSn for tissue of origin, DR5 for root meristems; Figs. 1, K to P, and 2A). After quality control, we obtained 3087 cells (893, 621, 445, and 1128 cells from the tissue of origin at stages 1, 3, and 5, respectively; mean unique molecular identifiers/cell = 5680; mean genes/cell = 2843).

Louvain clustering (*30*) of the combined data from all stages identified 13 clusters (Fig. 2B and fig. S3A). To annotate these, we applied the index of cell identity (ICI) method, based on the published expression profiles of seven tomato root tissues (*31*, *32*). Using 1669 identified marker genes (mean 273 markers/tissue; table S1), we obtained significant ICI classifications for 1861 cells [false discovery rate (FDR) < 0.05; fig. S3, B and C], identifying the xylem, phloem, stem cells, root cap, and vasculature initial clusters (clusters 3, 5, 8, 9, 10, and 2, respectively). A large number of cells were classified as root cortex parenchyma (clusters 1, 6, and 7), a tissue found in mature roots but absent from our microdissected tissues. Because these cells were enriched in the tissue of origin and stage 1 sorts (fig. S3A), we reasoned that they likely represented the morphologically similar phloem-associated parenchyma cells. To verify this, we generated a transcriptional reporter for *Solyc04g078650*, a tomato ortholog of the *Arabidopsis WOX4*, the expression of which was enriched in parenchyma clusters (fig. S3D; table S2), and that was previously reported to be expressed in tomato vasculature (*33*). Expression of *SlWOX4:mScarelti-NLS* was enriched in phloem parenchyma, and in situ hybridization revealed expression in phloem parenchyma and fibers (fig. S3, E to J). Among the *SlWOX4*-expressing parenchyma cells, cluster 6 specifically had mixed endodermis identity and was most abundant in stage 1 sort, which is enriched for distal phloem cells (Fig. 1K and fig. S3A). Although this root-specific tissue is not found in stems, this finding suggests the existence of multiple identities or cell states within the parenchyma tissue (fig. S3C). Cluster 11 consisted of cells from multiple and mixed identities. Common to these cells was high expression of G_1/S phase–associated cyclin A genes, suggesting that the cluster represents cells at this distinct stage of the cell cycle (fig. S3K).

Gene Ontology (GO) term analyses for the clusters' markers (FDR < 0.01; mean 969 markers/cluster; table S2), based either on annotation of tomato or of likely *Arabidopsis* orthologs, were consistent with the ICI identity assignments showing enrichment of phloem histogenesis terms. Markers for phloem parenchyma and distal phloem clusters were enriched for photosynthesis terms (figs. S4 and S5). Indeed, light can penetrate these external tissues and chloroplasts are found in distal phloem cells (fig. S1D). DNA replication and ribosome biogenesis terms were enriched in stem cells (figs. S4 and S5). Current annotation of shoot identities is sparse, and three clusters (12, 4, and 13) had ICI scores consistent with general vascular identity but could not be reliably assigned to a previously described cell type.

Root-specific identities such as root cap and procambium were only found from stage 3 onward, indicating that cells only differentiate at

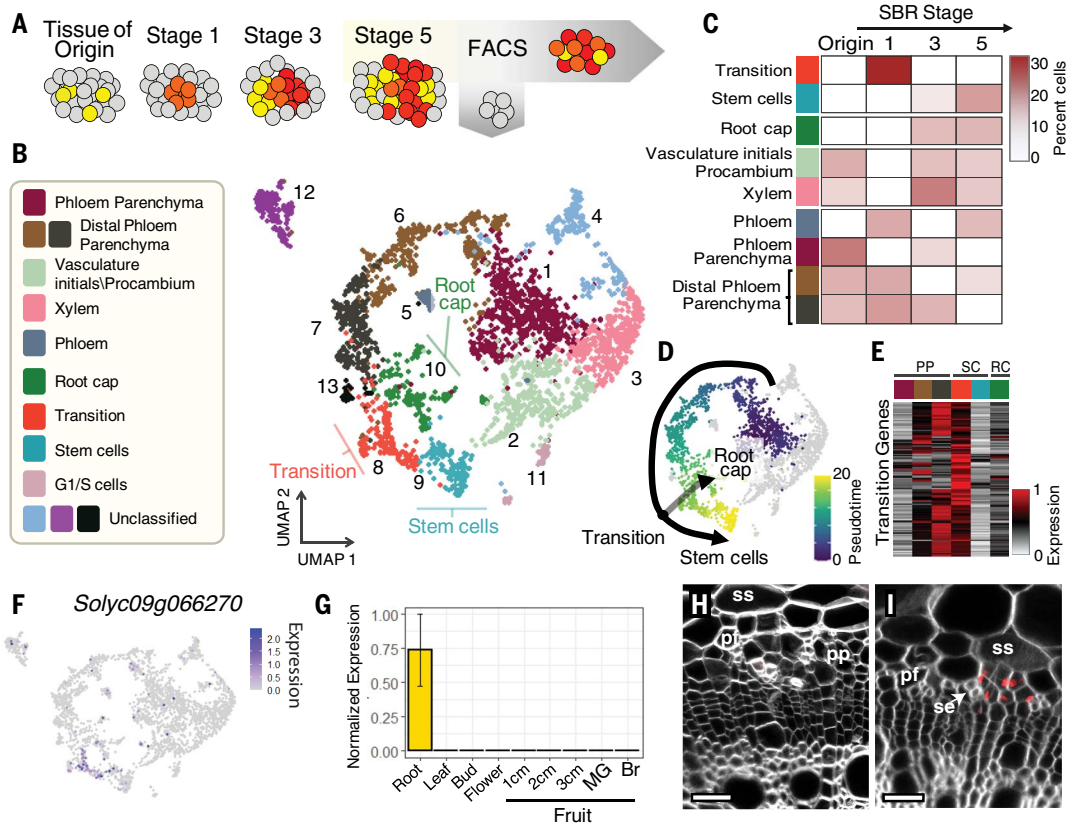

Fig. 2. Single-cell transcriptomics of shoot-borne root initiation. (**A**) Single-cell profiling experimental design. (**B**) Uniform manifold approximation and projection (UMAP) of cells from shoot-borne root development. (**C**) Composition of cell identities in each of the four stages expressed as a percentage of cells. (**D**) Trajectory of early stage identities. (**E**) Expression of transition genes along the phloem parenchyma to root trajectory. (**F** and **G**) Expression of *Solyc09g066270* from the single-cell data (F) and in the tomato expression atlas (*36*) (G). (**H** and **I**) Confocal images of *pSBRL:mScarleti-NLS-SBRLterm* in vascular tissue (H) and at stage 1 root meristems (I). Scale bars in (H) and (I), 25 μm.

later stages of meristem initiation. By contrast, one-third of stage 1 cells were classified as phloem parenchyma or phloem, confirming that shoot-borne roots arise from this tissue (Fig. 2C). Two clusters (8 and 9) were classified as stem cells and were enriched for the expression of several root stem cell regulators (fig. S6). One of the stem cell clusters was only found in stage 1, where it made up ~30% of the cells. A monocle3 (*34*) trajectory analysis identified this cluster as a branching point between root cap and the stem cells (clusters 9 and 10, respectively; Fig. 2D), suggesting that this ephemeral cell identity, which we named "transition," represents progenitors of the new shoot-borne root meristem. GO term enrichment for the two stem cell clusters was similar, but response to cytokinin and induction of the RNA interference machinery were unique to the transition cells. Overall, our single-cell analysis confirmed that shoot-borne roots arise from differentiated phloem parenchyma and identified a previously uncharacterized cell identity that is formed in the transition from phloem parenchyma to a root meristem.

SHOOTBORNE-ROOTLESS is required for root initiation

To identify potential regulators of transition stem cells, we searched for factors with expression that changed during the development from phloem parenchyma to stem cell and were enriched in transition compared with late-stage stem cells (FDR < 0.01). This included 128 genes (Fig. 2E), of which five were transcription factors: an AP2/ERF, two MYBs, a C2H2 zinc finger, and an LBD (fig. S7A). Expression of the tomato *WOX11* ortholog *Solyc06g072890* (*35*) was not detected at all in our dataset, suggesting that its shoot-borne root–specific function may not be conserved. One of the candidates, the LBD gene *Solyc09g066270*, was highly specific to transition cells and had root-specific expression in the tomato transcriptional atlas [(*36*); Fig. 2, F and G, and fig. S7B]. A transcriptional reporter confirmed this expression pattern (Fig. 2, H and I). *Solyc09g066270* is a class IB LBD (*37*), and members of this class were previously linked to the regulation of root development downstream of auxin (*17*). Injection of auxin into tomato internode 1 induced the expression of *Solyc09g066270*. This induction was abolished by cotreatment with auxin and cytokinin (fig. S7C), consistent with the inhibitory effect of prolonged cytokinin treatment on root initiation (*13*).

To characterize the function of *Solyc09g066270*, we used CRISPR to generate four independent null alleles (Fig. 3A and table S3). Mutants germinated normally, were fertile, and had normal shoot morphology (Fig. 3, B and C). However, all had barren stems and hypocotyls that completely lacked roots, even under flooding conditions that induce root emergence in wild-type (WT) tomato (*38*) (Fig. 3, D to G). When tomato stems are cut from the main root system, they readily form shoot-borne roots, but no such wound-induced roots formed in the mutant (Fig. 3, H and I). The hypocotyl has different ontogeny than the stem and is directly derived from embryonic tissue. Most of the wound-induced roots were lost in cut *sbrl* hypocotyls, but a small number of roots could still initiate from callus-like tissue formed at the wound site, indicating that these roots may be under distinct genetic regulation (Fig. 3, J and K, and fig. S8A). In accordance with its function, we named the gene *SHOOTBORNE-ROOTLESS* (*SBRL*). To determine whether the defect in *sbrl* mutants was in root initiation or emergence, we generated *sbrl DR5:VENUS-NLS* plants. We were unable to find *DR5*-expressing stage 1 or aberrant cell divisions in phloem tissue in six individual plants, suggesting that *SBRL* is specifically required for the earliest stage of root initiation (fig. S8, B and C).

Conservation of shoot-borne roots initiation program

The complete loss of shoot-borne roots in *sbrl* was reminiscent of the *rtcs* and *crl1* mutations in the distant monocots maize and rice, which are also caused by disruption to class IB LBD genes (*21*, *22*). To determine the evolutionary relationship between these genes, we generated a maximum likelihood tree of 845 class IB genes from 94 plant species [(*37*); table S4, Fig. 3L, and fig. S9]. This high-resolution analysis revealed that, rather than a single subclass, as

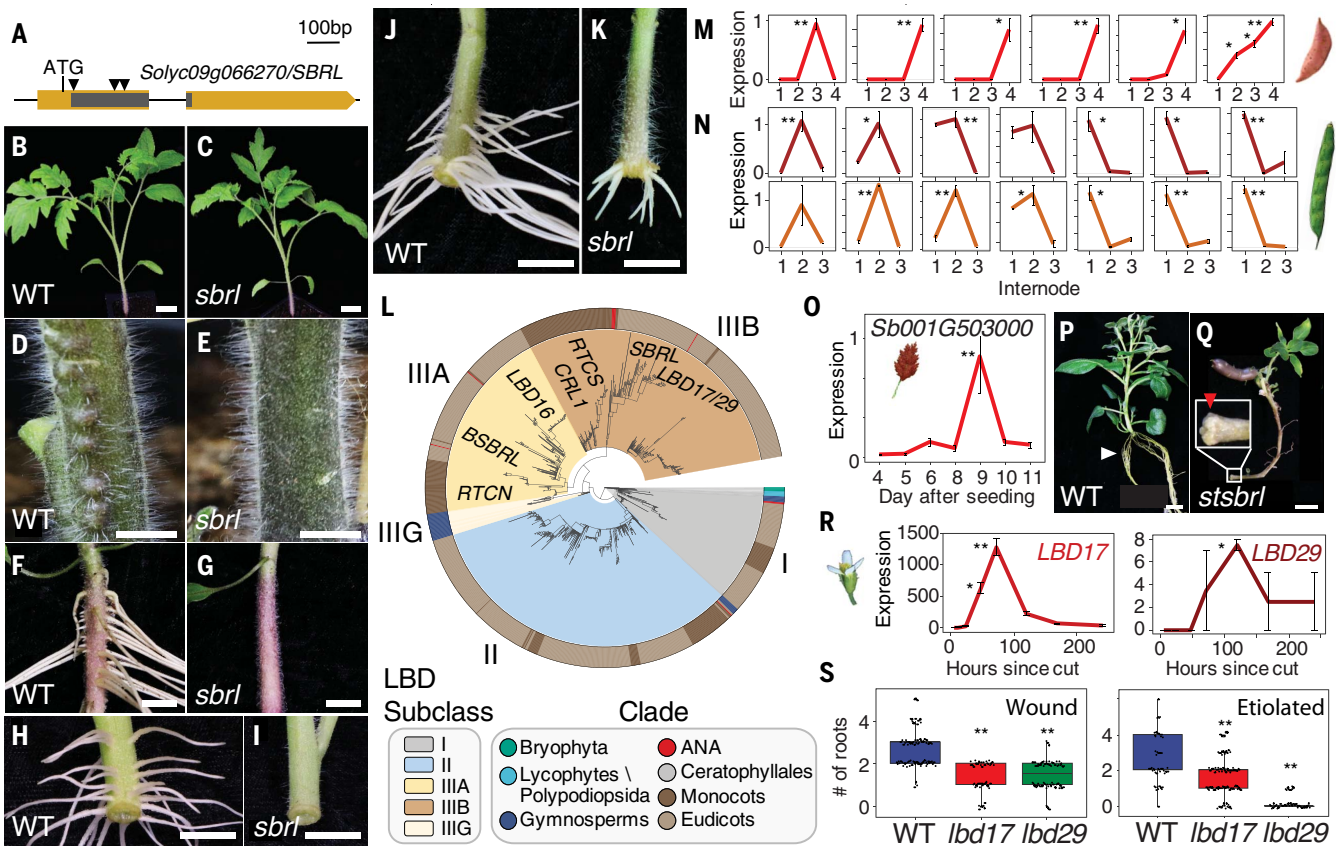

Fig. 3. *SBRL* regulates shoot-borne root initiation in angiosperms. (**A**) Structure of *SBRL*. The LBD is shown in gray. Arrowheads indicate guide RNA (gRNA) targets. (**B** and **C**) Four-week-old tomato plants. (**D** and **E**) First internode of 8-week-old tomato plants. (**F** and **G**) Four-week-old tomato hypocotyls after 1 week of flooding. (**H** to **K**) Cut first internode [(H) and (I)] or hypocotyls [(J) and (K)] 1 week after the cut. (**L**) Maximum likelihood tree of class IB LBDs. Branches with transfer bootstrap expectation < 0.7 were collapsed. See also high-resolution tree in fig S9. (**M** and **N**) Expression of the subclass IIIB genes *g15530* of *I. batatas* (M) and *Pv1G159400* (top) and *Pv7G19500* (bottom) of *P. vulgaris* (N). Each graph shows expression in stem sections of a single plant. In *I. batatas*, shoot-borne roots are apparent on node 5 or 6; in *P. vulgaris*, they are seen on internode 3 (see fig. S11). (**O**) Expression of class IIIB gene in the crown root region of *S. bicolor* (n = 4 or 5 for each time point). Crown roots appear after day 11 (see fig. S11). (**P** and **Q**) WT and *stsbrl* potato plants. White arrowhead marks shoot-borne roots, and red arrowhead marks the wound callus. *stsbrl* mutants are slow growing and develop tubers in culture, likely due to systemic effects. (**R**) Expression of *Arabidopsis* subclass IIIB genes in cut hypocotyls (*42*). (**S**) Number of roots formed on *Arabidopsis* hypocotyls after the removal of the root system (left) or induced by etiolation (right) (n = 95, 53, and 76 for WT, *lbd17*, and *lbd29* plants, respectively). Error bars indicate SE. Asterisks indicate statistical significant difference from baseline (WT or time 0 hour; *P < 0.05; **P < 0.001; Tukey's test). Scale bars in (B) to (K), (P), and (Q), 2 cm.

was previously reported (*37*), class IB LBDs form five distinct subclasses with subclass-specific protein motifs (fig. S10). Subclass I was found in ferns and all seed plants and likely represents the original member of the class. The moss and lycophytes genes were similar to subclass I but formed an outgroup to the five clades. Subclass II appeared in seed plants. Subclass III was divided into the gymnosperms-only subclass IIIG and the angiosperm-specific subclasses IIIA and IIIB. *SBRL*, *RTCS*, and *CRL1* were all classified as subclass IIIB (Fig. 3L).

Monocots and dicots are separated by ~150 million years (*39*), and both their vasculature anatomy and shoot-borne root physiology differ. That a mutation in a single subclass IIIB gene led to the loss of shoot-borne roots in all three species raised the hypothesis that the genetic regulation of these roots' initiation may be deeply conserved in plants. We tested whether the expression of subclass IIIB genes were induced during natural shoot-borne root initiation in two other dicots: sweet potato (*Ipomoea batatas*) and white bean (*Phaseolus vulgaris*). Shoot-borne root initiation could not be synchronized in these species, so we took advantage of the fact that roots formed a developmental gradient along the stem (fig. S11, A to N) and sampled the different stem sections of individual plants. Quantitative reverse transcription polymerase chain reaction (qRT-PCR) analysis showed that, in all cases, class IIIB genes were induced just before the morphological appearance of root meristems (Fig. 3, M and N). To test whether these expression patterns were conserved within monocots, we tested the expression of class IIIB genes during the initiation of *Sorghum bicolor* shoot-borne crown roots. As in dicots, a transient expression of this gene was detected before the morphological appearance of crown roots (Fig. 3O and fig. S11, O to R).

To determine whether the function of subclass IIIB is conserved, we generated CRISPR mutants in the potato (*Solanum tuberosum*) ortholog of *SBRL*, *StSBRL* (table S3). Potato readily generates shoot-borne roots when propagated in culture, but three independently derived CRISPR-homozygous mutants failed to form roots (Fig. 3, P and Q). *Arabidopsis* lacks elongated internodes but can form a few roots on its hypocotyl when it is cut from the main root system or when etiolated seedlings are exposed to light (*40*, *41*). Two close *SBRL Arabidopsis* homologs resulting from a Brassicaceae-specific duplication (LBD17/29)

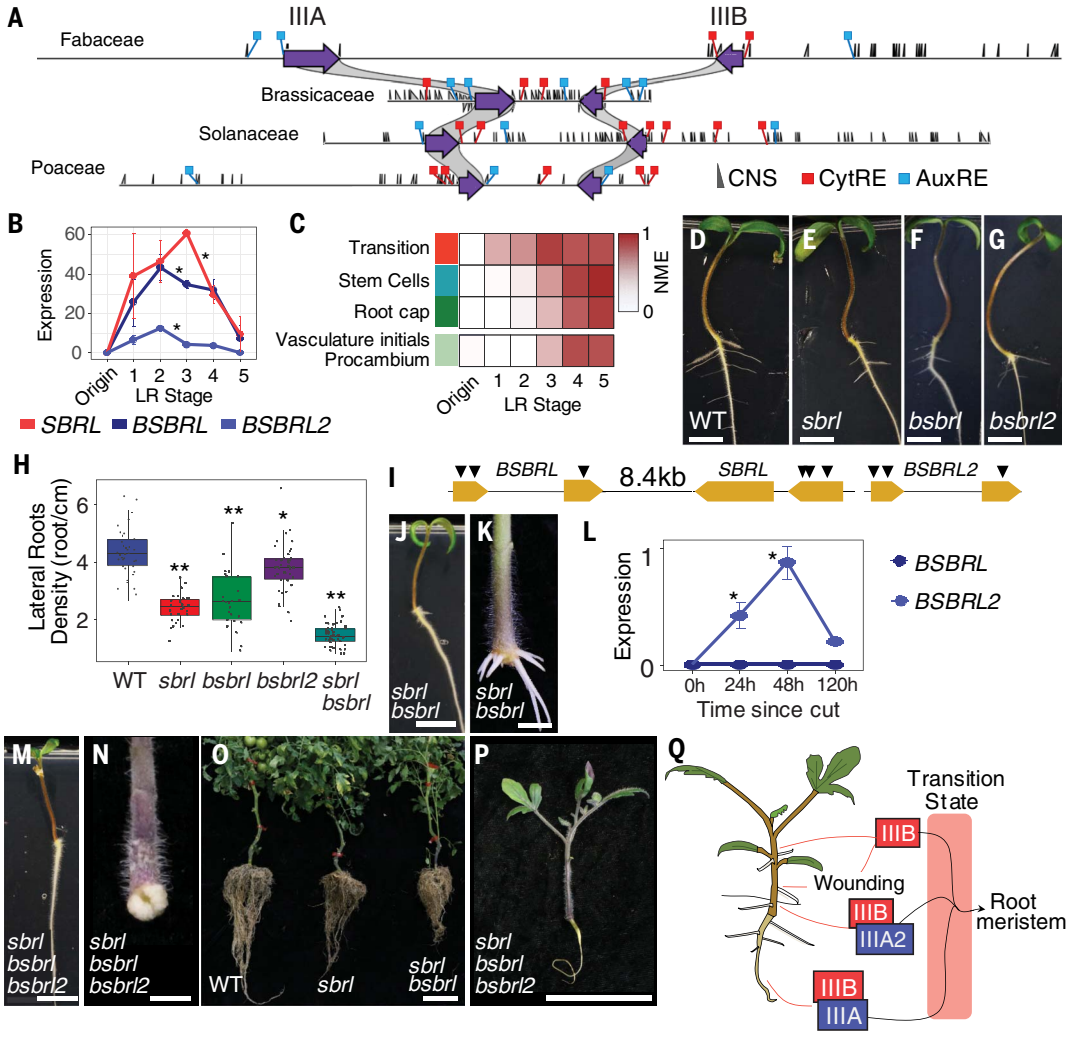

Fig. 4. A conserved superlocus regulates lateral root initiation. (**A**) Synteny and cis-regulatory sequence conservation in the *SBRL-BSBRL* superlocus. Black triangles mark conserved noncoding sequences. Red and blue squares mark conserved cytokinin and auxin response elements, respectively (CytRE: TGATTA; AuxRE: TGTCTC/CC/GG). (**B**) Expression of subclass IIIA/IIIB LBDs during tomato lateral root development. (**C**) Average expression of tissue identity markers during lateral root development. (**D** to **G**) Ten-day-old WT (D) and mutant [(E) to (G)] tomato seedlings. (**H**) Lateral root density in 10-day-old tomato seedlings (n = 50, 30, 25, 40, and 50 for WT, *sbrl*, *bsbrl*, *bsbrl2*, and *sbrl bsbrl*, respectively). (**I**) Gene structure of the *SBRL-BSBRL* superlocus and *BSBRL2*. Arrowheads mark gRNA targets. (**J** and **K**) Ten-day-old seedling (J) and cut hypocotyl 10 days after the cut (K) of *sbrl bsbrl* double mutants. (**L**) qRT-PCR expression of subclass IIIA genes during wound-induced root initiation on *sbrl* hypocotyl (n = 5). (**M** and **N**) Ten-day-old seedling (M) and cut hypocotyl 10 days after the cut (N) of *sbrl bsbrl bsbrl2* triple mutants. (**O** and **P**) Three-month-old pot-grown tomato plants. (**Q**) Model for the initiation of different root types in angiosperms. Error bars indicate SE. Asterisks indicate statistically significant difference from baseline (WT or time 0 hours; *P < 0.05; **P < 0.001). Data in (H) and (L) were analyzed with Tukey's test; data in (B) were analyzed by Welch's test. Scale bars: (D) to (G), (J), (K), (M), and (N), 1 cm; (O) and (P), 10 cm.

were transiently induced in the hypocotyl after removal of the root system [Fig. 3R; (*42*)]. Both CRISPR-generated null *lbd17* and *lbd29* mutants had reduced number of roots on cut hypocotyl. Similarly, both mutants exhibited a reduction in the number of roots developed on the hypocotyls of etiolated seedlings. However, *lbd29* mutants had a more significant reduction in the number of these roots (Fig. 3S and table S3; P < 0.001; Tukey's honestly significant difference), suggesting subfunctionalization of these paralogs. Finally, our hypothesis is supported by the evolutionary retention of subclass IIIB genes, because they were lacking only in three angiosperm species, two carnivorous plants, *Aldrovanda vesiculosa* and *Utricularia gibba*, and the water plant *Ceratophyllum demersum* (table S4). Common to all three is that they lost their roots during evolution. Taken together, our data indicate that the initiation program of shoot-borne roots and its specific regulation by subclass IIIB LBDs is deeply conserved in angiosperms.

Deep conservation of an LBD superlocus

During the assembly of the phylogenetic tree, we observed that subclass IIIB genes were almost always located immediately next to a closely related subclass IIIA gene in a single superlocus that exists already in basal-diverging angiosperms (fig. S13 and table S4). Cis-regulatory conservation analysis of 80 plant species from four families using the Conservatory algorithm (*43*), revealed broad conservation of noncoding regions within the locus, including multiple auxin and cytokinin response elements [Fig. 4A and table S5; (*28*)], supporting the existence of a conserved regulatory program for the entire locus. To test whether the function of this regulatory sequence is conserved, we constructed a dual reporter of the tomato regulatory sequences of *SBRL* and its syntenic subclass IIIA gene *BROTHER OF SBRL* (*BSBRL*; *pBSBRL:mNeonGreen-NLS-BSBRLterm pSBRL:mScarleti-NLS-SBRLterm*) and introduced it into *Arabidopsis*. Despite these species having diverged ~120 million years ago (*39*), the tomato regulatory sequence was sufficient to drive *mScarleti* expression in root primordia that formed on the *Arabidopsis* hypocotyl after removal of the root system (fig. S12, A to I).

The sequence similarity of subclass IIIA and IIIB genes suggests that they perform similar functions, but neither *BSBRL* nor its Solanaceae-specific duplication *BSBRL2* were detected in our single-cell expression dataset. *RTCN* and *LBD16*, the maize and *Arabidopsis* subclass IIIA genes (table S4), respectively, were previously linked to the regulation of lateral root development (*17*), suggesting that, similar to subclass IIIB function in shoot-borne roots, subclass IIIA genes may play a conserved role in lateral root initiation. To test

this hypothesis, we generated a transcriptional time series of tomato lateral root initiation (Fig. 1, Q to V, and fig. S14A). Both subclass IIIA and IIIB genes were transiently induced in initiating lateral roots, an expression pattern that was conserved in *I. batatas*, *P. vulgaris*, and *S. bicolor* (Fig. 4B and fig. S14, B to H). Furthermore, in *Arabidopsis*, the tomato regulatory sequence drove the transient coinduction of both markers in lateral root primorida. Some ectopic expression was observed in these lines, but because of technical limitations, only a subset of the conserved noncoding region in the 34-kb locus are present in our reporter (fig. S12, J to U). Regardless, these results confirm that the transient expression of subclass IIIA/IIIB gene in lateral root primorida and the core regulatory code driving it are deeply conserved.

To test whether the transient activation of subclass IIIA/IIIB LBD occurs within the context of a transition identity, we used the average expression of markers for the different shoot-borne root identities (table S2) to map the activation of each identity during lateral root development. Transition stem cell markers were the first to be induced, followed by markers of root cap, stem cells, and vasculature initials. This is consistent with the late acquisition of mature root cell identities that was recently reported in an analysis of *Arabidopsis* lateral root initiation (*44*). The sequence of identity transitions recapitulated that of shoot-borne roots, suggesting that subclass IIIA/IIIB may mediate similar processes in both cases (Fig. 4C).

Root-type-specific regulation by LBD genes

To test the functional role of subclass IIIA genes, we generated CRISPR mutants for tomato *bsbrl* and *bsbrl2*. Both these and *sbrl* mutants exhibited a mild but significant reduction in the number of lateral roots, as did mutants of the orthologous genes in *Arabidopsis* (Fig. 4, D to H; and fig. S14I; and table S3). By contrast, stems of both the *bsbrl* and *bsbrl2* mutants had normal shoot-borne root formation (fig. S14, J and K), and the number of roots forming on cut stems was not significantly different from that of WT (19 ± 1.4, 16.3 ± 3, and 19.4 ± 2.72 roots for WT, *bsbrl*, and *bsbrl2*, respectively; n = 6). To test whether the genes play a redundant function in lateral root initiation, we used a six-guide multiplex CRISPR to target the entire *SBRL-BSBRL* superlocus and examined four independently derived alleles (Fig. 4I and table S3). All *sbrl bsbrl* double mutants completely lacked shoot-borne roots and exhibited a significant reduction in the number of lateral roots, whereas the shoot remained unaffected (Fig. 4, H and J). Cut hypocotyl of the double mutant could still produce wound-induced roots (Fig. 4K). Time series expression analysis of these wound-induced hypocotyl roots in *sbrl* mutants revealed that the duplicated subclass IIIA gene *BSBRL2*, but not *BSBRL*, was transiently induced in this root type (Fig. 4L). To test whether these wound-induced roots are subclass IIIA/IIIB dependent, we generated a triple *sbrl bsbrl bsbrl2* mutant. Although slow to germinate, these plants formed normal primary embryonic roots (Fig. 4M; germinated at 2.6 ± 0.7 and 6.6 ± 1.1 days after sowing for WT and the triple mutant, respectively; n = 49 and 22). No wound-induced roots could form on cut hypocotyls of the triple mutant, with only callus-like cell proliferation apparent at the cut site (Fig. 4N). Furthermore, whereas the single and double *sbrl bsbrl* mutants could still develop a substantial branched root system when grown in soil (Fig. 4O), no postembryonic roots at all were developed in plants lacking the three subclass IIIA/IIIB genes, either when grown on plates or in soil (Fig. 4, M and P). Our data show that subclass IIIA/IIIB genes, which appeared in early angiosperms, are required for the initiation of postembryonic roots, with a conserved program driving individual paralogs to control root initiation in different developmental contexts.

It has been hypothesized that roots forming in different contexts differ in their early ontogeny but converge on a similar genetic program (*14*). Indeed, we show here that lateral and shoot-borne roots differ in terms of the number of initial cells involved and their hormonal dynamics. However, the data presented suggest a different model in which a common LBD-associated transition identity is shared among all root initiation events. We propose that the regulation of this common state by root-type-specific subclass IIIA/IIIB genes allows the specialization of different root types and thus is responsible for the diversity in root systems found in angiosperms (Fig. 4Q). Consistently, the initiation of nodules, a legume-specific lateral root-derived structure specialized for rhizobia interaction, is controlled by a legume-specific duplication of a subclass IIIA gene (*45*, *46*). The specific function of these genes and their conserved cis-regulatory program make them a prime target for the custom design of root system architectural traits.

Methods summary

Tomato [*S. lycopersicum* cultivar (cv) M82] seeds were germinated on soil, grown under 16-hour/8-hour light/dark conditions at 24°C for 6 weeks, and then transplanted to 10-liter pots in climate-controlled greenhouses (natural day length, 25°/20°C day/night temperature). *P. vulgaris* and *S. bicolor* were germinated in a closed, moist chamber at room temperatre, and 10-day-old seedlings were transferred to 5-liter pots in greenhouses. *I. batatas* cv Georgia Jet was grown from tubers in water at room temperature under ambient light. Seeds of *Arabidopsis* (Col-0) were grown on agar medium plates (0.5× Murashige and Skoog containing 0.5% sucrose and 0.8% agar), stratified for 3 days at 4°C in the dark, and transferred to a 16-/8-hour light/dark, 21°C growth chamber. CRISPR constructs were performed using plant codon–optimized Cas9 with up to six guide RNAs. Transgenic plants were created by cotyledon transformation for tomato, leaf explant transformation for *S. tuberosum* cv. Desirée, and floral dipping for *Arabidopsis*.

For single-cell analysis, cells from tomato internode 1 hand-dissected sections were dissociated in cell wall digestion solution for up to 1 hour, followed by cell separation using FACS into a 96-well plates. Collected RNA from 16 biological replicates was amplified, sequenced, and aligned to the ITAG4 genome with extended 3′ untranslated regions. Data normalization, scaling, and principal components analysis was performed with Seurat version 3 software using the default parameters. After batch and stage correction clusters were identified using the Louvain algorithm with multilevel refinement. Pseudotime trajectory analysis was performed using monocle3 (*34*) on cells from the parenchyma, stem cells, and root cap clusters. Identity classification were performed using ICI as previously described (*32*). GO term enrichment was performed using the goseq R package. GO terms with $P < 0.05$, as determined by the hypergeometric test, were considered significant.

In situ hybridization was performed using first internode of 4-week-old tomato plants. Antisense digoxigenin-labeled probes of SlWOX4 (Solyc04g078650) and the negative control H4 (Solyc04g011390), the expression of which was confined to the G_1/S phase, were produced by in vitro transcription.

For the phylogenetic analysis, class IB sequences were identified by searching the proteomes of all species for the canonical LBD class IB sequence (*37*). BLASTX was used to identify unannotated LBD transcripts. Protein sequences were aligned using MUSCLE, and the tree was constructed using IQ-tree2 with automatic model detection and 1000 bootstrap replicates. Conserved noncoding sequences were identified using Conservatory as described previously (*43*).

Transcriptional developmental series of tomato lateral root development was collected by manually dissecting 0.5-mm root slices from *DR5:3xVENUS-NLS* plants grown on agar plates. RNA was extracted from slices, followed by amplification and library preparation using the QuantSeq 3′ mRNA-Seq Library Prep Kit.

REFERENCE AND NOTES

1. J. J. Petricka, C. M. Winter, P. N. Benfey, Control of *Arabidopsis* root development. *Annu. Rev. Plant Biol.* **63**, 563–590 (2012). doi: 10.1146/annurev-arplant-042811-105501; pmid: 22404466
2. C. I. L. Peris, E. H. Rademacher, D. Weijers, Green beginnings - pattern formation in the early plant embryo. *Curr. Top. Dev. Biol.* **91**, 1–27 (2010). doi: 10.1016/S0070-2153(10)91001-6; pmid: 20705177

3. K. Sugimoto, S. P. Gordon, E. M. Meyerowitz, Regeneration in plants and animals: Dedifferentiation, transdifferentiation, or just differentiation? *Trends Cell Biol.* **21**, 212–218 (2011). doi: 10.1016/j.tcb.2010.12.004; pmid: 21236679
4. G. Wachsman, J. Zhang, M. A. Moreno-Risueno, C. T. Anderson, P. N. Benfey, Cell wall remodeling and vesicle trafficking mediate the root clock in *Arabidopsis*. *Science* **370**, 819–823 (2020). doi: 10.1126/science.abb7250; pmid: 33184208
5. W. Xuan *et al*., Cyclic programmed cell death stimulates hormone signaling and root development in *Arabidopsis*. *Science* **351**, 384–387 (2016). doi: 10.1126/science.aad2776; pmid: 26798015
6. T. van den Berg *et al*., A reflux-and-growth mechanism explains oscillatory patterning of lateral root branching sites. *Dev. Cell* **56**, 2176–2191.e10 (2021). doi: 10.1016/j.devcel.2021.07.005; pmid: 34343477
7. I. De Smet *et al*., Auxin-dependent regulation of lateral root positioning in the basal meristem of *Arabidopsis*. *Development* **134**, 681–690 (2007). doi: 10.1242/dev.02753; pmid: 17215297
8. M. A. Moreno-Risueno *et al*., Oscillating gene expression determines competence for periodic *Arabidopsis* root branching. *Science* **329**, 1306–1311 (2010). doi: 10.1126/science.1191937; pmid: 20829477
9. A. J. Dickinson *et al*., A plant lipocalin promotes retinal-mediated oscillatory lateral root initiation. *Science* **373**, 1532–1536 (2021). doi: 10.1126/science.abf7461; pmid: 34446443
10. K. Esau, *Anatomy of Seed Plants* (Wiley, 1977).
11. A. J. Hetherington, L. Dolan, Evolution: Diversification of angiosperm rooting systems in the Early Cretaceous. *Curr. Biol.* **29**, R1081–R1083 (2019). doi: 10.1016/j.cub.2019.08.030; pmid: 31639353
12. P. Groff, D. R. Kaplan, The relation of root systems to shoot systems in vascular plants. *Bot. Rev.* **54**, 387–422 (1988). doi: 10.1007/BF02858417
13. C. Bellini, D. I. I. Pacurar, I. Perrone, Adventitious roots and lateral roots: Similarities and differences. *Annu. Rev. Plant Biol.* **65**, 639–666 (2014). doi: 10.1146/annurev-arplant-050213-035645; pmid: 24555710
14. K. D. Birnbaum, How many ways are there to make a root? *Curr. Opin. Plant Biol.* **34**, 61–67 (2016). doi: 10.1016/j.pbi.2016.10.001; pmid: 27780106
15. L. Chang, E. Ramireddy, T. Schmülling, Cytokinin as a positional cue regulating lateral root spacing in *Arabidopsis*. *J. Exp. Bot.* **66**, 4759–4768 (2015). doi: 10.1093/jxb/erv252; pmid: 26019251
16. A. Bielach *et al*., Spatiotemporal regulation of lateral root organogenesis in *Arabidopsis* by cytokinin. *Plant Cell* **24**, 3967–3981 (2012). doi: 10.1105/tpc.112.103044; pmid: 23054471
17. J. Lavenus *et al*., Lateral root development in *Arabidopsis*: Fifty shades of auxin. *Trends Plant Sci.* **18**, 450–458 (2013). doi: 10.1016/j.tplants.2013.04.006; pmid: 23701908
18. C. Galinha *et al*., PLETHORA proteins as dose-dependent master regulators of *Arabidopsis* root development. *Nature* **449**, 1053–1057 (2007). doi: 10.1038/nature06206; pmid: 17960244
19. Y. Du, B. Scheres, Lateral root formation and the multiple roles of auxin. *J. Exp. Bot.* **69**, 155–167 (2018). doi: 10.1093/jxb/erx223; pmid: 28992266
20. H. Hofhuis *et al*., Phyllotaxis and rhizotaxis in *Arabidopsis* are modified by three PLETHORA transcription factors. *Curr. Biol.* **23**, 956–962 (2013). doi: 10.1016/j.cub.2013.04.048; pmid: 23684976
21. G. Taramino *et al*., The maize (*Zea mays* L.) RTCS gene encodes a LOB domain protein that is a key regulator of embryonic seminal and post-embryonic shoot-borne root initiation. *Plant J.* **50**, 649–659 (2007). doi: 10.1111/j.1365-313X.2007.03075.x; pmid: 17425722
22. Y. Inukai *et al*., Crown rootless1, which is essential for crown root formation in rice, is a target of an AUXIN RESPONSE FACTOR in auxin signaling. *Plant Cell* **17**, 1387–1396 (2005). doi: 10.1105/tpc.105.030981; pmid: 15829602
23. H. Liu *et al*., ARL1, a LOB-domain protein required for adventitious root formation in rice. *Plant J.* **43**, 47–56 (2005). doi: 10.1111/j.1365-313X.2005.02434.x; pmid: 15960615
24. Y. Kitomi *et al*., The auxin responsive AP2/ERF transcription factor CROWN ROOTLESS5 is involved in crown root initiation in rice through the induction of OsRR1, a type-A response regulator of cytokinin signaling. *Plant J.* **67**, 472–484 (2011). doi: 10.1111/j.1365-313X.2011.04610.x; pmid: 21481033
25. Y. Zhao, Y. Hu, M. Dai, L. Huang, D.-X. Zhou, The WUSCHEL-related homeobox gene WOX11 is required to activate shoot-borne crown root development in rice. *Plant Cell* **21**, 736–748 (2009). doi: 10.1105/tpc.108.061655; pmid: 19258439
26. T. Ulmasov, Z. B. Liu, G. Hagen, T. J. Guilfoyle, Composite structure of auxin response elements. *Plant Cell* **7**, 1611–1623 (1995). pmid: 7580254
27. E. Zürcher *et al*., A robust and sensitive synthetic sensor to monitor the transcriptional output of the cytokinin signaling network in planta. *Plant Physiol.* **161**, 1066–1075 (2013). doi: 10.1104/pp.112.211763; pmid: 23355633
28. M. Lieberman-Lazarovich, C. Yahav, A. Israeli, I. Efroni, Deep conservation of *cis*-element variants regulating plant hormonal responses. *Plant Cell* **31**, 2559–2572 (2019). doi: 10.1105/tpc.19.00129; pmid: 31467248
29. B. Müller, J. Sheen, Cytokinin and auxin interaction in root stem-cell specification during early embryogenesis. *Nature* **453**, 1094–1097 (2008). doi: 10.1038/nature06943; pmid: 18463635
30. T. Stuart *et al*., Comprehensive integration of single-cell data. *Cell* **177**, 1888–1902.e21 (2019). doi: 10.1016/j.cell.2019.05.031; pmid: 31178118
31. K. Kajala *et al*., Innovation, conservation, and repurposing of gene function in root cell type development. *Cell* **184**, 3333–3348.e19 (2021). doi: 10.1016/j.cell.2021.04.024; pmid: 34010619
32. I. Efroni, P.-L. Ip, T. Nawy, A. Mello, K. D. Birnbaum, Quantification of cell identity from single-cell gene expression profiles. *Genome Biol.* **16**, 9 (2015). doi: 10.1186/s13059-015-0580-x; pmid: 25608970
33. J. Ji *et al*., WOX4 promotes procambial development. *Plant Physiol.* **152**, 1346–1356 (2010). doi: 10.1104/pp.109.149641; pmid: 20044450
34. J. Cao *et al*., The single-cell transcriptional landscape of mammalian organogenesis. *Nature* **566**, 496–502 (2019). doi: 10.1038/s41586-019-0969-x; pmid: 30787437
35. C. Wang *et al*., The WOX family transcriptional regulator SILAM1 controls compound leaf and floral organ development in *Solanum lycopersicum*. *J. Exp. Bot.* **72**, 1822–1835 (2021). doi: 10.1093/jxb/eraa574; pmid: 33277994
36. Tomato Genome Consortium, The tomato genome sequence provides insights into fleshy fruit evolution. *Nature* **485**, 635–641 (2012). doi: 10.1038/nature11119; pmid: 22660326
37. A. S. Chanderbali, F. He, P. S. Soltis, D. E. Soltis, Out of the water: Origin and diversification of the LBD gene family. *Mol. Biol. Evol.* **32**, 1996–2000 (2015). doi: 10.1093/molbev/msv080; pmid: 25839188
38. M. L. Vidoz, E. Loreti, A. Mensuali, A. Alpi, P. Perata, Hormonal interplay during adventitious root formation in flooded tomato plants. *Plant J.* **63**, 551–562 (2010). doi: 10.1111/j.1365-313X.2010.04262.x; pmid: 20497380
39. S. Kumar, G. Stecher, M. Suleski, S. B. Hedges, TimeTree: A resource for timelines, timetrees, and divergence times. *Mol. Biol. Evol.* **34**, 1812–1819 (2017). doi: 10.1093/molbev/msx116; pmid: 28387841
40. P. Sukumar, G. S. Maloney, G. K. Muday, Localized induction of the ATP-binding cassette B19 auxin transporter enhances adventitious root formation in *Arabidopsis*. *Plant Physiol.* **162**, 1392–1405 (2013). doi: 10.1104/pp.113.217174; pmid: 23677937
41. C. Sorin *et al*., Auxin and light control of adventitious rooting in *Arabidopsis* require ARGONAUTE1. *Plant Cell* **17**, 1343–1359 (2005). doi: 10.1105/tpc.105.031625; pmid: 15829601
42. C. W. Melnyk *et al*., Transcriptome dynamics at *Arabidopsis* graft junctions reveal an intertissue recognition mechanism that activates vascular regeneration. *Proc. Natl. Acad. Sci. U.S.A.* **115**, E2447–E2456 (2018). doi: 10.1073/pnas.1718263115; pmid: 29440499
43. A. Hendelman *et al*., Conserved pleiotropy of an ancient plant homeobox gene uncovered by cis-regulatory dissection. *Cell* **184**, 1724–1739.e16 (2021). doi: 10.1016/j.cell.2021.02.001; pmid: 33667348
44. L. Serrano-Ron *et al*., Reconstruction of lateral root formation through single-cell RNA sequencing reveals order of tissue initiation. *Mol. Plant* **14**, 1362–1378 (2021). pmid: 34062316
45. T. Soyano, Y. Shimoda, M. Kawaguchi, M. Hayashi, A shared gene drives lateral root development and root nodule symbiosis pathways in *Lotus*. *Science* **366**, 1021–1023 (2019). doi: 10.1126/science.aax2153; pmid: 31754003
46. K. Schiessl *et al*., NODULE INCEPTION recruits the lateral root develop4mental program for symbiotic nodule organogenesis in *Medicago truncatula*. *Curr. Biol.* **29**, 3657–3668.e5 (2019). doi: 10.1016/j.cub.2019.09.005; pmid: 31543454

ACKNOWLEDGMENTS

We thank T. Beeckman, Y. Eshed, Z. Lippman, and S. Savaldi-Goldstein for comments and discussions; M. De Martino for setting up the CRISPR system; I. Pri-Tal for tissue culture work; O. Roth for assistance in etiolated seedlings assay; and M. Chemla for assistance in library preparation. **Funding:** I.E. is supported by a Howard Hughes Medical Institute International Research Scholar grant (grant no. 55008730) and the Israeli Science Foundation (grant no. ISF966/17). A.H. is supported by National Science Foundation grant Plant Genome Research Program grant IOS-1546837 to Z.B.L. **Author contributions:** M.O., N.G.-Y., and I.E. conceived and designed the study and performed the experiments. C.Y. performed the shoot-borne root quantification and lateral root RNA-Seq assay. A.H. performed in situ hybridizations. E.S. performed potato transformation. I.E., N.G.-Y., and M.O. wrote the manuscript. **Competing interests:** The authors declare no competing interests. **Data and materials availability:** Raw and processed data are available at the Gene Expression Omnibus (GEO; single-cell data: GSE159055; lateral root transcriptome data: GSE159050). All other data are available in the main paper or the supplementary materials.

SUPPLEMENTARY MATERIALS

science.org/doi/10.1126/science.abf4368
Materials and Methods
Figs. S1 to S14
References (*47*–*68*)
Tables S1 to S6
MDAR Reproducibility Checklist

View/request a protocol for this paper from *Bio-protocol*.

2 November 2020; resubmitted 17 October 2021
Accepted 13 January 2022
10.1126/science.abf4368